

# Simulation of Random Fields via Local Average Subdivision

BY GORDON A. FENTON AND ERIK H. VANMARCKE<sup>1</sup>, Members, ASCE

## *Abstract*

A fast and accurate method of generating realizations of a homogeneous Gaussian scalar random process in one, two, or three dimensions is presented. The resulting discrete process represents local averages of a homogeneous random function defined by its mean and covariance function, the averaging being performed over incremental domains formed by different levels of discretization of the field. The approach is motivated first by the need to represent engineering properties as local averages (since many properties are not well defined at a point and show significant scale effects), and second to be able to easily condition the realization to incorporate known data or change resolution within sub-regions. The ability to condition the realization or increase the resolution in certain regions is an important contribution to finite element modeling of random phenomena. The Ornstein-Uhlenbeck and fractional Gaussian noise processes are used as illustrations.

## **Introduction**

Stochastic models of natural phenomena are rapidly gaining popularity within the scientific community for a variety of reasons, not the least of which is marked improvements in computer processing speeds and graphics capabilities. From a predictive point of view, the major use of such models is in the quantification of system reliability and optimization of data acquisition. Many problems of practical interest to engineers remain unsolved by analytical means but are amenable to approximate solutions via Monte Carlo simulation. In the context of stochastic finite element analyses, Monte Carlo techniques are intuitively appealing and often give good results for otherwise intractable problems.

In this paper a fast and accurate method of producing realizations of a discrete ‘local average’ random process is presented. The motivation for such an approach arose out of a need to account for the fact that most engineering measurements are only defined over some finite domain and thus represent a local average of the property. For example, soil porosity is ill-defined at the micro-scale – it is measured using samples of finite volume and the variability of the values obtained is often significantly effected by the volume tested. The same is true of strength measurements, say concrete cylinders, or radar measurements of cloud or rainfall densities (see also Rodriguez-Iturbe

---

<sup>1</sup> Graduate student and Professor, Dept. of Civil Engineering and Operations Research, Princeton University, NJ 08544

1986). A properly defined random local average process is therefore more easily related to actual measurements made at any scale and those measures more easily incorporated.

Another advantage to the proposed method is that it is ideally suited to stochastic finite element modeling using efficient, low order, interpolation functions. Each discrete local average given by a realization becomes the average property within each discrete element. In this context, the ability to easily change the resolution of a region of the domain while maintaining internal consistency will give finite element modelers the freedom of changing mesh resolution in regions of interest.

The concept behind the Local Average Subdivision (LAS) approach arose out of the stochastic subdivision algorithm described by Carpenter (1980) and Fournier *et al.* (1982). Their method was limited to modeling power spectra having a  $\omega^{-\beta}$  form and suffered from problems with aliasing and ‘creasing’. Lewis (1987) generalized the approach to allow the modeling of arbitrary power spectra without eliminating the aliasing. Such midpoint displacement algorithms involve recursively subdividing the domain by generating new midpoint values randomly selected according to some distribution. Once chosen, the value at a point remains fixed and at each stage in the subdivision only half the points in the process are determined (the others created in previous iterations). Aliasing arises because the power spectral density is not modified at each stage to reflect the increasing Nyquist frequency associated with each increase in resolution. Voss (in Peitgen *et al.* 1988, Chap. 1) attempted to eliminate this problem with considerable success by adding randomness to all points at each stage in the subdivision in a method called ‘successive random additions’. However the internal consistency easily achieved by the midpoint displacement methods (their ability to return to previous states while decreasing resolution through decimation) is largely lost with the successive random additions technique. The property of internal consistency in the midpoint displacement approaches implies that certain points retain their value throughout the subdivision and other points are created to remain consistent with them with respect to correlation. In the LAS approach, internal consistency implies that certain regions maintain a constant average throughout the subdivision. The property of internal consistency is important because it allows the process to be easily conditioned.

The method proposed here solves the problems associated with the stochastic subdivision methods and incorporates into it concepts of local averaging theory. The general concept and procedure is presented first for a one-dimensional stationary process characterized by its second-order statistics. The algorithm is illustrated by a Ornstein-Uhlenbeck process, having a simple exponential correlation function, as well as by a fractional Gaussian noise process as defined by Mandelbrot and van Ness (1968). The simulation procedure in two and three dimensions is then described. Finally some comments concerning the relative efficiency of the method are made.

## One-Dimensional Local Average Subdivision

The construction of a local average process via LAS essentially proceeds in a top-down recursive fashion (Fenton 1990) as illustrated in Figure 1. In Stage 0, a global average is generated for the process. In Stage 1, the domain is subdivided into two regions whose ‘local’ averages must in turn average to the global (or parent) value. Subsequent stages are obtained by subdividing each ‘parent’ cell and generating values for the resulting two regions while preserving upwards averaging. Note that the global average remains constant throughout the subdivision, a property that is ensured merely by requiring that the average of each pair generated is equivalent to the parent cell value. This is also a property of any cell being subdivided – such internal consistency allows for simple conditioning of the process. Specifically, the algorithm proceeds as follows;

- 1) generate a normally distributed global average (labeled  $Z_1^0$  in Figure 1) with mean zero and variance obtained from local averaging theory,
- 2) subdivide the field into two equal parts,
- 3) generate two normally distributed values,  $Z_1^1$  and  $Z_2^1$ , whose means and variances are selected so as to satisfy three criteria:
  - a) that they show the correct variance according to local averaging theory,
  - b) that they are properly correlated with one another,
  - c) that they average to the parent value,  $\frac{1}{2}(Z_1^1 + Z_2^1) = Z_1^0$ .

That is, the distributions of  $Z_1^1$  and  $Z_2^1$  are conditioned on the value of  $Z_1^0$ ,

- 4) subdivide each cell in stage 1 into two equal parts,
- 5) generate two normally distributed values,  $Z_1^2$  and  $Z_2^2$ , whose means and variances are selected so as to satisfy four criteria:
  - a) that they show the correct variance according to local averaging theory,
  - b) that they are properly correlated with one another,
  - c) that they average to the parent value,  $\frac{1}{2}(Z_1^2 + Z_2^2) = Z_1^1$ ,
  - d) that they are properly correlated with  $Z_3^2$  and  $Z_4^2$ .

The third criteria implies conditioning of the distributions of  $Z_1^2$  and  $Z_2^2$  on the value of  $Z_1^1$ .

The fourth criteria will only be satisfied approximately by conditioning their distributions also on  $Z_2^1$ .

and so on in this fashion. The approximations in the algorithm come about in two ways: first the correlation with adjacent cells across parent boundaries is accomplished through the parent values (which are already known having been previously generated). Second the range of parent cells on which to condition the distributions will be limited to some neighborhood. The remainder of this paper is devoted largely to the determination of these conditional Gaussian distributions at each

stage in the subdivision and to an estimation of the algorithmic errors. In the following, the term ‘parent cell’ refers to the previous stage cell being subdivided and ‘within-cell’ means within the region defined by the parent cell.

To determine the mean and variance of the Stage 0 value,  $Z_1^0$ , consider first a continuous stationary scalar random function  $Z(t)$  in one dimension, a sample of which may appear as shown in Figure 2, and define a domain of interest  $(0, D]$  within which a realization is to be produced. Two comments should be made at this point: First, as it is currently implemented the method is restricted to stationary processes fully described by their second-order statistics (mean, variance and autocorrelation function or, equivalently, spectral density function). This is not a severe restriction since it leaves a sufficiently broad class of functions to model most natural phenomena (Lewis 1987); also, there is often insufficient data to substantiate more complex probabilistic models. Second, the subdivision procedure depends on the physical size of the domain being defined since the dimension over which local averaging is to be performed must be known. The process  $Z$  beyond the domain  $(0, D]$  is ignored.

The average of  $Z(t)$  over the domain  $(0, D]$  is given by

$$Z_1^0 = \frac{1}{D} \int_0^D Z(\xi) d\xi \quad (1)$$

where  $Z_1^0$  is a random variable whose statistics

$$E [Z_1^0] = E [Z] \quad (2)$$

$$E [(Z_1^0)^2] = \left(\frac{1}{D^2}\right) \int_0^D \int_0^D E [Z(\xi) Z(\xi')] d\xi d\xi' = E [Z]^2 + \left(\frac{2}{D^2}\right) \int_0^D (D - \tau) B(\tau) d\tau \quad (3)$$

can be found by making use of stationarity and the fact that  $B(\tau)$ , the covariance function of  $Z(t)$ , is an even function of lag  $\tau$ . Without loss in generality,  $E [Z]$  will henceforth be taken as zero where  $E [\cdot]$  is the expectation operator. If  $Z(t)$  is a Gaussian random function, (2) and (3) give sufficient information to generate a realization of  $Z_1^0$  which becomes stage 0 in the LAS method. If  $Z(t)$  is not Gaussian, then the complete probability distribution function for  $Z_1^0$  must be determined and a realization generated according to such a distribution. This is beyond the scope of the present paper and so we restrict our attention to Gaussian processes.

Consider now the general case where stage  $i$  is known and stage  $i + 1$  is to be generated. In the following the superscript  $i$  denotes the stage under consideration. Define

$$D^i = \frac{D}{2^i}, \quad i = 0, 1, 2, \dots, L, \quad (4)$$

where the desired number of intervals in the realization is  $N = 2^L$ , and define  $Z_k^i$  to be the average of  $Z(t)$  over the interval  $(k-1)D^i < t \leq kD^i$  centered at  $t_k = (k - \frac{1}{2})D^i$ , i.e.

$$Z_k^i = \frac{1}{D^i} \int_{(k-1)D^i}^{kD^i} Z(\xi) d\xi \quad (5)$$

where  $E[Z_k^i] = E[Z] = 0$ . The target covariance between local averages separated by lag  $mD^i$  between centers is

$$\begin{aligned} E[Z_k^i Z_{k+m}^i] &= E \left[ \left( \frac{1}{D^i} \right)^2 \int_{(k-1)D^i}^{kD^i} \int_{(k+m-1)D^i}^{(k+m)D^i} Z(\xi) Z(\xi') d\xi d\xi' \right] \\ &= \left( \frac{1}{D^i} \right)^2 \int_0^{D^i} \int_{mD^i}^{(m+1)D^i} B(\xi - \xi') d\xi d\xi' \\ &= \left( \frac{1}{D^i} \right)^2 \int_{(m-1)D^i}^{mD^i} (\xi - (m-1)D^i) B(\xi) d\xi + \left( \frac{1}{D^i} \right)^2 \int_{mD^i}^{(m+1)D^i} ((m+1)D^i - \xi) B(\xi) d\xi. \end{aligned} \quad (6)$$

A much simpler formulation is possible by introducing the concept of a variance function defined as follows (Vanmarcke 1984)

$$\gamma^{(D^i)} = \left( \frac{1}{\sigma D^i} \right)^2 \int_0^{D^i} \int_0^{D^i} B(\xi - \xi') d\xi d\xi' = 2 \left( \frac{1}{\sigma D^i} \right)^2 \int_0^{D^i} (|D^i| - |\tau|) B(\tau) d\tau \quad (7)$$

where  $\sigma^2 = B(0)$ . Vanmarcke has determined this function for a variety of processes. In terms of the variance function, (6) becomes

$$E[Z_k^i Z_{k+m}^i] = \frac{\sigma^2}{2} \left[ (m-1)^2 \gamma((m-1)D^i) - 2m^2 \gamma(mD^i) + (m+1)^2 \gamma((m+1)D^i) \right] \quad (8)$$

With reference to Figure 3, the construction of stage  $i+1$  given stage  $i$  is obtained by estimating a mean for  $Z_{2j}^{i+1}$  and adding a zero mean discrete white noise  $c^{i+1} U_j^{i+1}$  having variance  $(c^{i+1})^2$

$$Z_{2j}^{i+1} = M_{2j}^{i+1} + c^{i+1} U_j^{i+1}. \quad (9)$$

The best linear estimate for the mean  $M_{2j}^{i+1}$  can be determined by a linear combination of stage  $i$  (parent) values in some neighborhood  $j-n, \dots, j+n$ ,

$$M_{2j}^{i+1} = \sum_{k=j-n}^{j+n} a_{k-j}^i Z_k^i. \quad (10)$$

Multiplying (9) through by  $Z_m^i$ , taking expectations and using the fact that  $U_j^{i+1}$  is uncorrelated with the stage  $i$  values allows the determination of the coefficients  $a$  in terms of the desired covariances,

$$\mathbf{E} [Z_{2j}^{i+1} Z_m^i] = \sum_{k=j-n}^{j+n} a_{k-j}^i \mathbf{E} [Z_k^i Z_m^i] \quad (11)$$

a system of equations ( $m = j - n, \dots, j + n$ ) from which the coefficients  $a_\ell^i$ ,  $\ell = -n, \dots, n$ , can be solved. The covariance matrix multiplying the vector  $\{a_\ell^i\}$  is both symmetric and Toeplitz (elements along each diagonal are equal). For  $U_j^{i+1} \sim N(0, 1)$  the variance of the noise term is  $(c^{i+1})^2$  which can be obtained by squaring (9), taking expectations and employing the results of (11)

$$(c^{i+1})^2 = \mathbf{E} [(Z_{2j}^{i+1})^2] - \sum_{k=j-n}^{j+n} a_{k-j}^i \mathbf{E} [Z_{2j}^{i+1} Z_k^i]. \quad (12)$$

The adjacent cell,  $Z_{2j-1}^{i+1}$ , is determined by ensuring that upwards averaging is preserved – that the average of each stage  $i + 1$  pair equals the value of the stage  $i$  parent,

$$Z_{2j-1}^{i+1} = 2 Z_j^i - Z_{2j}^{i+1} \quad (13)$$

which incidentally gives a means of evaluating the cross-stage covariances

$$\mathbf{E} [Z_{2j}^{i+1} Z_m^i] = \frac{1}{2} \mathbf{E} [Z_{2j}^{i+1} Z_{2m-1}^{i+1}] + \frac{1}{2} \mathbf{E} [Z_{2j}^{i+1} Z_{2m}^{i+1}]. \quad (14)$$

All the expectations in Equations (11) to (14) are evaluated using (6) or (8) at the appropriate stage.

For stationary processes, the set of coefficients  $\{a_\ell^i\}$  and  $c^i$  are independent of position since the expectations in (11) and (12) are just dependent on lags. The generation procedure can be restated as follows;

- 1) for  $i = 0, 1, 2, \dots, L$  compute the coefficients  $\{a_\ell^i\}$ ,  $\ell = -n, \dots, n$  using (11) and  $c^{i+1}$  using (12),
- 2) starting with  $i = 0$ , generate a realization for the global mean using (2) and (3),
- 3) subdivide the domain,
- 4) for each  $j = 1, 2, \dots, 2^i$ , generate realizations for  $Z_{2j}^{i+1}$  and  $Z_{2j-1}^{i+1}$  using (9) and (13),
- 5) increment  $i$  and, if not greater than  $L$ , return to step 3.

Notice that subsequent realizations of the process need only start at step 2 and so the overhead involved with setting up the coefficients becomes rapidly negligible.

Because the LAS procedure is recursive, obtaining stage  $i + 1$  values using the previous stage, it is relatively easy to condition the field simply by specifying the values of the local averages at a

particular stage. So, for example, if the global mean of a process is known *a priori*, then the stage 0 value can be set to this mean and the LAS procedure started at stage 1. Similarly if the resolution is to be refined in a certain region, then the values in that region become the starting values and the subdivision resumed at the next stage.

Although the LAS method yields a local average process, when the discretization size becomes small enough it is virtually indistinguishable from the limiting continuous process. Thus the method can be used to approximate continuous functions as well.

### Accuracy

It is instructive to investigate how closely the algorithm approximates the target statistics of the process. Changing notation slightly, denote the stage  $i + 1$  algorithmic values, given the stage  $i$  values, as

$$\hat{Z}_{2j}^{i+1} = c^{i+1} U_j^{i+1} + \sum_{k=j-n}^{j+n} a_{k-j}^i Z_k^i \quad (15)$$

$$\hat{Z}_{2j-1}^{i+1} = 2 Z_j^i - \hat{Z}_{2j}^{i+1}. \quad (16)$$

It is easy to see that the expectation of  $\hat{Z}$  is still zero, as desired, while the variance is

$$\begin{aligned} \mathbf{E} [(\hat{Z}_{2j}^{i+1})^2] &= \mathbf{E} \left[ \left( c^{i+1} U_j^{i+1} + \sum_{k=j-n}^{j+n} a_{k-j}^i Z_k^i \right)^2 \right] \\ &= (c^{i+1})^2 + \sum_{k=j-n}^{j+n} a_{k-j}^i \sum_{\ell=j-n}^{j+n} a_{\ell-j}^i \mathbf{E} [Z_k^i Z_\ell^i] \\ &= \mathbf{E} [(Z_{2j}^{i+1})^2] - \sum_{k=j-n}^{j+n} a_{k-j}^i \mathbf{E} [Z_{2j}^{i+1} Z_k^i] + \sum_{k=j-n}^{j+n} a_{k-j}^i \mathbf{E} [Z_{2j}^{i+1} Z_k^i] \\ &= \mathbf{E} [(Z_{2j}^{i+1})^2] \end{aligned} \quad (17)$$

in which the coefficients  $c^{i+1}$  and  $a_\ell^i$  were calculated using (11) and (12) as before. Similarly, the within-cell covariance at lag  $D^{i+1}$  is

$$\mathbf{E} [\hat{Z}_{2j-1}^{i+1} \hat{Z}_{2j}^{i+1}] = \mathbf{E} \left[ \left( 2 Z_j^i - c^{i+1} U_j^{i+1} - \sum_{k=j-n}^{j+n} a_{k-j}^i Z_k^i \right) \left( c^{i+1} U_j^{i+1} + \sum_{\ell=j-n}^{j+n} a_{\ell-j}^i Z_\ell^i \right) \right]$$

$$\begin{aligned}
&= 2 \sum_{\ell=j-n}^{j+n} a_{\ell-j}^i \mathbf{E} [Z_{\ell}^i Z_j^i] - \mathbf{E} [(Z_{2j}^{i+1})^2] \\
&= 2 \mathbf{E} [Z_{2j}^{i+1} Z_j^i] - \mathbf{E} [(Z_{2j}^{i+1})^2] \\
&= \mathbf{E} [Z_{2j-1}^{i+1} Z_{2j}^{i+1}]
\end{aligned} \tag{18}$$

using the results of (17) along with (14). Thus the covariance structure within a cell is preserved *exactly* by the subdivision algorithm. Some approximation does occur across cell boundaries as can be seen by considering

$$\begin{aligned}
\mathbf{E} [\hat{Z}_{2j}^{i+1} \hat{Z}_{2j+1}^{i+1}] &= \mathbf{E} \left[ \left( c^{i+1} U_j^{i+1} + \sum_{k=j-n}^{j+n} a_{k-j}^i Z_k^i \right) \left( 2 Z_{j+1}^i - c^{i+1} U_{j+1}^{i+1} - \sum_{\ell=j-n+1}^{j+n+1} a_{\ell-j-1}^i Z_{\ell}^i \right) \right] \\
&= 2 \sum_{k=j-n}^{j+n} a_{k-j}^i \mathbf{E} [Z_k^i Z_{j+1}^i] - \sum_{\ell=j-n+1}^{j+n+1} a_{\ell-j-1}^i \sum_{k=j-n}^{j+n} a_{k-j}^i \mathbf{E} [Z_k^i Z_{\ell}^i] \\
&= \mathbf{E} [Z_{2j}^{i+1} Z_{2j+1}^{i+1}] + \mathbf{E} [Z_{2j}^{i+1} Z_{2j+2}^{i+1}] - \sum_{\ell=j-n+1}^{j+n+1} a_{\ell-j-1}^i \mathbf{E} [Z_{2j}^{i+1} Z_{\ell}^i]
\end{aligned} \tag{19}$$

The algorithmic error in this covariance comes from the last two terms. The discrepancy between (19) and the exact covariance is illustrated numerically in Figure 4 for a zero mean Ornstein-Uhlenbeck process having covariance and variance functions

$$B(\tau) = \sigma^2 \exp \left\{ -\frac{2|\tau|}{\theta} \right\} \tag{20}$$

$$\gamma(T) = \frac{\theta^2}{2T^2} \left[ \frac{2|T|}{\theta} + \exp \left\{ \frac{-2|T|}{\theta} \right\} - 1 \right] \tag{21}$$

where  $T$  is the averaging dimension (in Figure 4,  $T = D^{i+1}$ ) and  $\theta$  is the scale of fluctuation of the process. The exact covariance is determined by (8) (for  $m = 1$ ) using the variance function (21). Although Figure 4 shows a wide range in the effective cell sizes,  $2T/\theta$ , the error is typically very small.

To address the issue of errors at larger lags and the possibility of errors accumulating from stage to stage, it is useful to look at the exact versus estimated statistics of the entire process. Figure 5 illustrates this comparison for the Ornstein-Uhlenbeck process. It can be seen from this example and from the fractional Gaussian noise example to come, that the errors are self-correcting and the algorithmic correlation structure tends to the exact correlation function when averaged over several realizations. Spectral analysis of realizations obtained from the LAS method show equally good agreement between estimated and exact (Fenton 1990). The within-cell rate of convergence of the estimated statistics to the exact is  $1/N_f$ , where  $N_f$  is the number of realizations. The overall rate of convergence is about the same.

## Boundary Conditions and Neighborhood Size

When the neighborhood size  $(2n + 1)$  is greater than 1 ( $n > 0$ ), the construction of values near the boundary may require values from the previous stage which lie outside the boundary. This problem is handled by assuming that what happens outside the domain  $(0, D]$  is of no interest and uncorrelated with what happens within the domain. The generating relationship (9) near either boundary becomes

$$Z_{2j}^{i+1} = c^{i+1} U_j^{i+1} + \sum_{k=j-p}^{j+q} a_{k-j}^i Z_k^i \quad (22)$$

where  $p = \min(n, j - 1)$ ,  $q = \min(n, 2^i - j)$  and the coefficients  $a_\ell^i$  need only be determined for  $\ell = -p, \dots, q$ . The periodic boundary conditions mentioned by Lewis (1987) are not appropriate if the target covariance structure is to be preserved since they lead to a covariance which is symmetric about lag  $D/2$  (unless the desired covariance is also symmetric about this lag).

In the implementation described in this paper, a neighborhood size of 3 was used ( $n = 1$ ), the parent cell plus its two adjacent cells. Because of the top-down approach, there seems to be little justification to using a larger neighborhood for processes with covariance functions which decrease monotonically or which are relatively smooth. When the covariance function is oscillatory, a larger neighborhood is required in order to successfully approximate the function. In Figure 6 the exact and estimated covariances are shown for a process with

$$B(\tau) = \sigma^2 \cos(\omega\tau) e^{-2\tau/\theta}. \quad (23)$$

Considerable improvement in the model is obtained when a neighborhood size of 5 is used ( $n = 2$ ). This improvement comes at the expense of taking about twice as long to generate the realizations. Many practical models of natural phenomena employ monotonically decreasing covariance functions, often for simplicity, and so the  $n = 1$  implementation is usually preferable.

## Fractional Gaussian Noise

As a further demonstration of the LAS method, a self-similar process called fractional Gaussian noise was simulated. Fractional Gaussian noise (fGn) is defined by Mandelbrot *et al.* [5] to be the derivative of fractional Brownian motion (fBm), obtained by averaging the fBm over a small interval  $\delta$ . The resulting process has covariance and variance functions

$$B(\tau) = \frac{\sigma^2}{2\delta^{2H}} \left[ |\tau + \delta|^{2H} - 2|\tau|^{2H} + |\tau - \delta|^{2H} \right] \quad (24)$$

$$\gamma(T) = \frac{|T + \delta|^{2H+2} - 2|T|^{2H+2} + |T - \delta|^{2H+2} - 2\delta^{2H+2}}{T^2(2H + 1)(2H + 2)\delta^{2H}} \quad (25)$$

defined for  $0 < H < 1$ . The case  $H = 0.5$  corresponds to white noise and  $H \rightarrow 1$  gives  $\omega^{-1}$  type noise. In practice  $\delta$  is taken to be equal to the smallest lag between field points ( $\delta = D/2^L$ ) to ensure that when  $H = 0.5$  (white noise),  $B(\tau)$  becomes zero for all  $\tau \geq D/2^L$ . A sample function and its corresponding ensemble statistics are shown in Figure 7 for  $\omega^{-\beta}$  type noise ( $H = 0.95$ ) where  $\beta = 2H - 1$ . The self-similar type processes have been demonstrated by Mandelbrot (1982), Voss (1985), and many others (Mohr 1981, Peitgen *et al.* 1988, Whittle 1956, to name a few) to be representative of a large variety of natural forms and patterns, for example music, terrains, crop yields, and chaotic systems.

## Multi-Dimensional Extensions

In two dimensions, a rectangular domain is defined and the subdivision proceeds by dividing rectangles into 4 equal areas at each stage. In order to preserve the exact within-cell covariance structure, three random noises are added to three of the quadrants and the fourth quadrant is determined such that upwards averaging is preserved. Figure 8 presents the 2-D LAS scheme for the first 3 stages in which the center of each local average is marked with a different symbol for each stage. The generating relationships are,

$$\begin{aligned}
Z_1^{i+1} &= Z_{2j,2k}^{i+1} &= c_{11}^{i+1} U_{1jk}^{i+1} + \sum_{\ell=1}^{n_{xy}} a_{\ell 1}^i Z_{m(\ell),n(\ell)}^i \\
Z_2^{i+1} &= Z_{2j,2k-1}^{i+1} &= c_{21}^{i+1} U_{1jk}^{i+1} + c_{22}^{i+1} U_{2jk}^{i+1} + \sum_{\ell=1}^{n_{xy}} a_{\ell 2}^i Z_{m(\ell),n(\ell)}^i \\
Z_3^{i+1} &= Z_{2j-1,2k}^{i+1} &= c_{31}^{i+1} U_{1jk}^{i+1} + c_{32}^{i+1} U_{2jk}^{i+1} + c_{33}^{i+1} U_{3jk}^{i+1} + \sum_{\ell=1}^{n_{xy}} a_{\ell 3}^i Z_{m(\ell),n(\ell)}^i \\
Z_4^{i+1} &= Z_{2j-1,2k-1}^{i+1} &= 4Z_{jk}^i - Z_{2j,2k}^{i+1} - Z_{2j,2k-1}^{i+1} - Z_{2j-1,2k}^{i+1}
\end{aligned} \tag{26}$$

where  $U$  is a Gaussian variate with zero mean and unit variance and  $m(\ell)$ ,  $n(\ell)$  are indexing functions traversing (in a fixed pattern) the  $n_{xy} = (2n_x + 1) \times (2n_y + 1)$  neighborhood of  $Z_{jk}^i$ . In this implementation,  $n_x = n_y = 1$  and the boundary conditions are handled in the same fashion as for the 1-D case. The coefficients  $\{a_{\ell r}^i\}$  can be calculated from the linear equations

$$\begin{aligned}
\mathbb{E} [Z_{2j,2k}^{i+1} Z_{m(p),n(p)}^i] &= \sum_{\ell=1}^{n_{xy}} a_{\ell 1}^i \mathbb{E} [Z_{m(\ell),n(\ell)}^i Z_{m(p),n(p)}^i], & p = 1, 2, \dots, n_{xy} \\
\mathbb{E} [Z_{2j,2k-1}^{i+1} Z_{m(p),n(p)}^i] &= \sum_{\ell=1}^{n_{xy}} a_{\ell 2}^i \mathbb{E} [Z_{m(\ell),n(\ell)}^i Z_{m(p),n(p)}^i], & p = 1, 2, \dots, n_{xy}
\end{aligned} \tag{27}$$

$$\mathbf{E} [Z_{2j-1,2k}^{i+1} Z_{m(p),n(p)}^i] = \sum_{\ell=1}^{n_{xy}} a_{\ell 3}^i \mathbf{E} [Z_{m(\ell),n(\ell)}^i Z_{m(p),n(p)}^i], \quad p = 1, 2, \dots, n_{xy}$$

in which the matrices on the right hand sides are symmetric but no longer Toeplitz in general. The coefficient matrix  $\mathbf{c}^{i+1}$  is assumed to be lower triangular satisfying

$$\mathbf{c}^{i+1} \cdot (\mathbf{c}^{i+1})^T = \mathbf{R} \quad (28)$$

where  $\mathbf{R}$  is symmetric and given by

$$R_{rs} = \mathbf{E} [Z_r^{i+1} Z_s^{i+1}] - \sum_{\ell=1}^{n_{xy}} a_{\ell r}^i \mathbf{E} [Z_{m(\ell),n(\ell)}^i Z_s^{i+1}] \quad r, s = 1, 2, 3 \quad (29)$$

using the indexing notation defined at the extreme left of (26). The assumption of homogeneity vastly decreases the number of coefficients that need to be calculated and stored since  $\{a_{\ell r}^i\}$  and  $\mathbf{c}^{i+1}$  become independent of position. As in the 1-D case, the coefficients need only be calculated prior to the first realization – they can be re-used in subsequent realizations reducing the effective cost of their calculation.

The expectations used in equations (27) to (29) can be determined from the two dimensional variance function of the process

$$\mathbf{E} [Z_{jk}^i Z_{j+m,k+n}^i] = \frac{1}{4}\sigma^2 \sum_{p=-1}^1 w_p(m+p)^2 \sum_{q=-1}^1 w_q(n+q)^2 \gamma((m+q)D_x^i, (n+p)D_y^i) \quad (30)$$

where,

$$w_\ell = \begin{cases} -2, & \text{when } \ell = 0 \\ 1, & \text{otherwise} \end{cases}$$

and where  $D_x^i$  and  $D_y^i$  are the dimensions of the individual averaging rectangles at stage  $i$ . For a quadrant symmetric covariance structure,  $\gamma(\cdot)$  is defined by Vanmarcke (1984) to be

$$\gamma(T_1, T_2) = \left(\frac{1}{\sigma T_1 T_2}\right)^2 \int_{-T_1}^{T_1} \int_{-T_2}^{T_2} (|T_1| - |\tau_1|)(|T_2| - |\tau_2|) B(\tau_1, \tau_2) d\tau_1 d\tau_2 \quad (31)$$

A sample function of a  $5 \times 5$  first-order Markov process having isotropic covariance function

$$B(\tau_1, \tau_2) = \sigma^2 \exp\left\{-\frac{2}{\theta} \sqrt{\tau_1^2 + \tau_2^2}\right\} \quad (32)$$

was generated using the two-dimensional LAS algorithm and is shown in Figure 9. The field was subdivided 8 times to obtain a  $256 \times 256$  resolution giving relatively small cells of size  $\frac{5}{256} \times \frac{5}{256}$ .

The estimated covariances along three different directions are seen in Figure 10 to show very good agreement with the exact (30). The agreement improves (as  $1/N_f$ ) when the statistics are averaged over a larger number of realizations. Notice that the horizontal axis on Figure 10 extends beyond a lag of 5 to accommodate the estimation of the covariance along the diagonal (which has length  $5\sqrt{2}$ ).

In three dimensions, the LAS method involves recursively subdividing rectangular parallelepipeds into 8 equal volumes at each stage. The generating relationships are essentially the same as in the 2-D case except now 7 random noises are used in the subdivision of each parent volume at each stage

$$Z_s^{i+1} = \sum_{r=1}^s c_{rs}^{i+1} U_{sjkl}^{i+1} + \sum_{\ell=1}^{n_{xyz}} a_{\ell s}^i Z_{m(\ell),n(\ell),p(\ell)}^i \quad s = 1, 2, \dots, 7 \quad (33)$$

$$Z_8^{i+1} = 8Z_{jkl}^i - \sum_{s=1}^7 Z_s^{i+1} \quad (34)$$

in which  $Z_s^{i+1}$  denotes a particular octant of the subdivided cell centered at  $Z_{jkl}^i$ . For a neighborhood size,  $n_{xyz}$ , of  $3 \times 3 \times 3$ , Figure 11 compares the estimated and exact covariance of a three-dimensional first-order Markov process having isotropic covariance

$$B(\tau_1, \tau_2, \tau_3) = \sigma^2 \exp\left\{-\frac{2}{\theta} \sqrt{\tau_1^2 + \tau_2^2 + \tau_3^2}\right\} \quad (35)$$

The physical field size of  $5 \times 5 \times 5$  was subdivided 6 times to obtain a resolution of  $64 \times 64 \times 64$  and the covariance estimates were averaged over 50 realizations.

## Implementation and Efficiency

In order to calculate stage  $i + 1$  values, the values at stage  $i$  must be known. This implies that in the 1-D case, storage must be provided for at least  $1.5N$  values where  $N = 2^L$  is the desired number of intervals of the process. The implementation described in this paper stores all the previous stages, a storage requirement of  $(2N - 1)$  in 1-D,  $\frac{4}{3}(N \times N)$  in 2-D, and  $\frac{8}{7}(N \times N \times N)$  in 3-D. This allows rapid ‘zooming out’ of the field. The coefficients  $\{a^i\}$  and  $c^i$ , which must also be stored, can be efficiently calculated using LU factorization (see Equation 28) and successive backsubstitutions (see Equation 27). The Toeplitz property of the matrix in Equation (11) was not taken advantage of for neighborhood sizes greater than 3.

The LAS method is also very competitive with the popular Fast Fourier Transform method in its execution speed. Table 1 compares times of the two methods running on a Cyber 205 (CDC) super-computer for one, two, and three-dimensional realizations. In one dimension, using

a neighborhood size of 3, LAS runs slightly faster than the FFT approach. Both methods have negligible setup times for the coefficient calculations. In two and three dimensions, the LAS approach runs about 1.5 to 2 times slower than the FFT. One needs to be careful in making a direct comparison, however, since the FFT approach yields an observed covariance structure which is symmetric about  $D/2$  due to assumed periodicity (Fenton 1990). Thus to obtain a process with the correct statistics via FFT, the size of the field must be increased (and the excess ignored), in some cases by as much as a factor of 2. This means that execution times of a ‘corrected’ FFT method could be as much as  $2^E$  times greater than those shown in Table 1, where  $E$  is the dimension of the process.

## Conclusions

The LAS algorithm has been found to be an efficient and accurate means of producing realizations of homogeneous Gaussian random local average processes in one, two or three dimensions. The primary advantages the method has over existing approaches are;

- 1) conditioning the realization using known local averages is simple,
- 2) produces realizations which are scale dependent and show the proper covariance between local averages at any resolution,
- 3) ideally suited to finite element models using efficient low order interpolation functions in which each local average becomes an element property,
- 4) avoids the aliasing, creasing, and symmetric covariance problems found with other traditional methods.

As it is currently implemented, the method is restricted to isotropic covariance functions in 2 and 3 dimensions. This is not a serious restriction since anisotropic fields having ellipsoidal covariance functions can be simply produced by scaling the space coordinates of an isotropic process appropriately.

## Acknowledgements

The authors would like to thank the John von Neumann National Supercomputer Center for their support of this work under Grant LAC-21023. Additional support was made available by the National Science Foundation under Grant ECE-8611521 and by the National Center for Earthquake Engineering Research under NCEER Project 88-3004. Any opinions, findings, and conclusions or recommendations are those of the authors and do not necessarily reflect the views of the above-mentioned organizations.

## Appendix I. References

- CARPENTER, L. C., (1980). "Computer Rendering of Fractal Curves and Surfaces", *ACM Computer Graphics*, SIGGRAPH 80 Proceedings, pg. 109.
- FENTON, G. A., (1990). *Simulation and Analysis of Random Fields*, Ph.D. Thesis, Dept. of Civ. Engrg. and Op. Research, Princeton University, Princeton, NJ.
- FOURNIER, A., FUSSELL, D., and CARPENTER, L., (1982). "Computer Rendering of Stochastic Models", *Communications of the ACM*, **25**(6), 371–384.
- LEWIS, J. P., (1987). "Generalized Stochastic Subdivision", *ACM Transactions on Graphics*, **6**(3), 167–190.
- MANDELBROT, B. B., and VAN NESS, J. W., (1968). "Fractional Brownian Motion, Fractional Noises and Applications", *SIAM Review*, **10**(4), 422–437.
- MANDELBROT, B. B., (1982). *The Fractal Geometry of Nature*, W.H. Freeman and Co., New York, NY.
- MOHR, D. L., (1981). *Modeling Data as a Fractional Gaussian Noise*, Ph.D. Thesis, Dept. of Statistics, Princeton University, Princeton, NJ.
- PEITGEN, H-O, and SAUPE, D., Ed. (1988). *The Science of Fractal Images*, Springer-Verlag, New York, NY.
- RODRIGUEZ-ITURBE, I., (1986). "Scale of Fluctuation of Rainfall Models", *Water Resources Research*, **22**(9), 15S–37S.
- VANMARCKE, E. H., (1984). *Random Fields: Analysis and Synthesis*, The MIT Press, Cambridge, Massachusetts.
- VOSS, R. F., (1985). "Random Fractal Forgeries", in *Fundamental Algorithms for Computer Graphics*, R. A. Earnshaw, ed., Springer-Verlag, Berlin, 805–835.
- WHITTLE, P., (1956). "On the Variation of Yield Variance with Plot Size", *Biometrika*, **43**, 343–343.

## Appendix II. Notations

The following symbols are used in this paper:

$$\beta = 2H - 1$$

$\delta$  = interval over which fBm is averaged in order to define the derivative

$\gamma(\cdot)$  = variance function of the process  $Z$

$\theta$  = scale of fluctuation

$\sigma$  = standard deviation of the continuous point process  $Z$

$\tau$  = lag

$\omega$  = frequency, radians/sec

$a_k^i$  = best linear estimate coefficient at stage  $i$

$B(\cdot)$  = covariance function of  $Z$

$c^i$  = coefficients of the noise  $U$  at stage  $i$

$D$  = physical length of process

$D^i$  = physical length of a cell of the subdivided field at stage  $i$

$E[\cdot]$  = expectation operator

$H$  = self-similarity parameter

$L$  = desired number of subdivisions to perform

$M$  = estimated mean

$N$  = desired number of elements in the final process

$N_f$  = number of realizations of the field

$n$  = neighborhood range

$U$  = unit variance, zero mean discrete Gaussian white noise

$Z$  = scalar random function

$Z_k^i$  = average of  $Z$  over length  $D^i$  centered at  $(k - \frac{1}{2})D^i$

$\hat{Z}_k^i$  = algorithmic approximation to  $Z_k^i$

### *List of Figure Captions*

- FIG. 1 Top-down approach to the LAS construction of a local average random process.
- FIG. 2 Realization of a continuous random function  $Z$  with a domain of interest  $(0, D]$  defined.
- FIG. 3 One-dimensional LAS indexing for stage  $i$  (top) and stage  $i + 1$  (bottom).
- FIG. 4 Comparison of algorithmic and exact correlation between adjacent cells across a parent cell boundary for varying effective cell dimensions  $2T/\theta$ .
- FIG. 5 Comparison of the exact and estimated (averaged over 200 realizations) covariance functions of the Ornstein-Uhlenbeck process (20) with  $\sigma = 1$  and scale of fluctuation  $\theta = 4$ .
- FIG. 6 Effect of neighborhood size for (a)  $n = 1$  and (b)  $n = 2$  on the estimated covariance of damped oscillatory noise (23) produced by the LAS method.
- FIG. 7 LAS generated sample function of  $\omega^{-\beta}$  noise for  $H = 0.95$  (a) and corresponding estimated (averaged over 200 realizations) versus exact covariance function (b).
- FIG. 8 First three stages and indexing scheme of the 2-D LAS algorithm (stage 0 =  $\boxtimes$ , stage 1 = +, and stage 2 =  $\circ$ ).
- FIG. 9 LAS generated sample function of the two-dimensional first-order Markov process (32) for  $\theta = \frac{1}{2}$ .
- FIG. 10 Comparison of exact and estimated (averaged over 100 realizations) covariance functions of the two-dimensional first-order Markov process (32) with  $\sigma = 1$  and  $\theta = \frac{1}{2}$ .
- FIG. 11 Comparison of exact and estimated (averaged over 50 realizations) covariance functions of the three-dimensional first-order Markov process (35) with  $\sigma = 1$  and  $\theta = 4$ . Dashed lines show estimates in various directions through the volume.

## **Summary**

A fast and accurate method of simulating homogeneous Gaussian scalar random processes in one, two, or three dimensions is presented. Realizations are made up of discrete local averages of the underlying random field which are consistent with the level of resolution and which can be easily conditioned. Theoretical basis for the procedure is discussed and several examples are presented involving one-, two-, and three-dimensional random fields.

## **Keywords**

simulation, random processes, stochastic models, probability, statistics, Monte-Carlo, fractional Gaussian noise, random fields, stochastic finite elements.

**Table 1 Comparison of execution times on a Cyber 205 super-computer**

Type	Resolution	Number of Realizations	Time (seconds)	
			Setup	Generation
1-D FFT	256	200	0.0013	0.18
1-D LAS	256	200	0.0017	0.15
2-D FFT	256×256	100	0.1265	15.20
2-D LAS	256×256	100	0.1156	23.01
3-D FFT	64×64×64	50	0.1517	48.77
3-D LAS	64×64×64	50	6.1740	100.57

Stage 0	$Z_1^0$							
Stage 1	$Z_1^1$				$Z_2^1$			
Stage 2	$Z_1^2$		$Z_2^2$		$Z_3^2$		$Z_4^2$	
Stage 3	$Z_1^3$	$Z_2^3$	$Z_3^3$	$Z_4^3$	$Z_5^3$	$Z_6^3$	$Z_7^3$	$Z_8^3$
Stage 4								

Figure 1 (Fenton/VanMarcke)

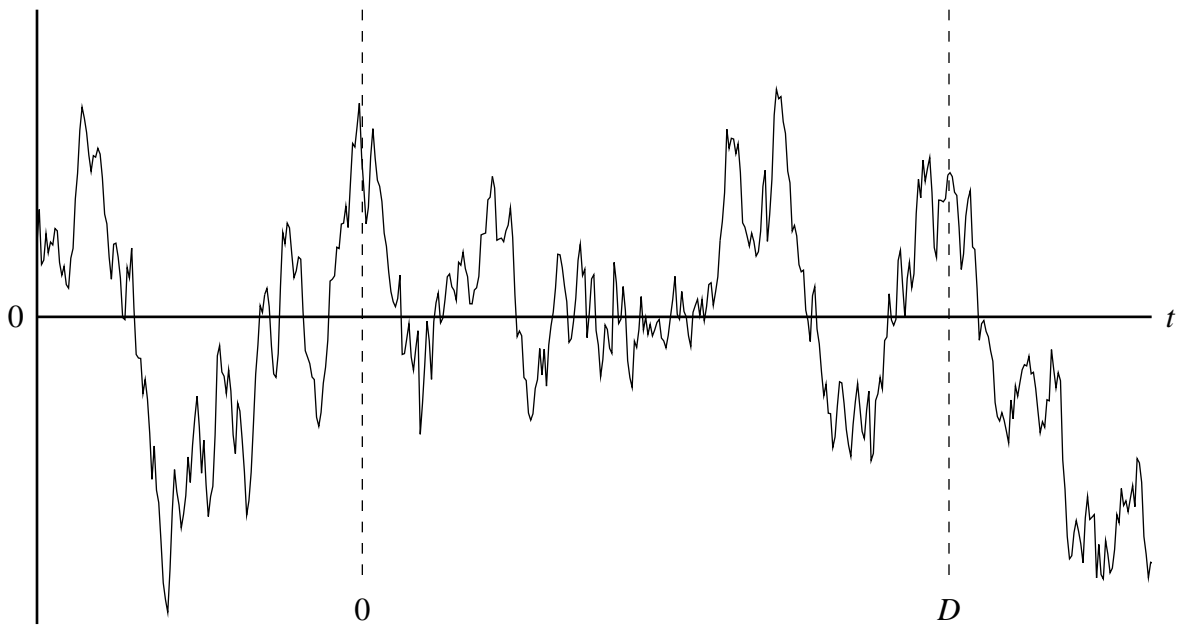


Figure 2 (Fenton/VanMarcke)

	$j$		$j+1$		
	$2j-1$	$2j$	$2j+1$	$2j+2$	

Figure 3 (Fenton/VanMarcke)

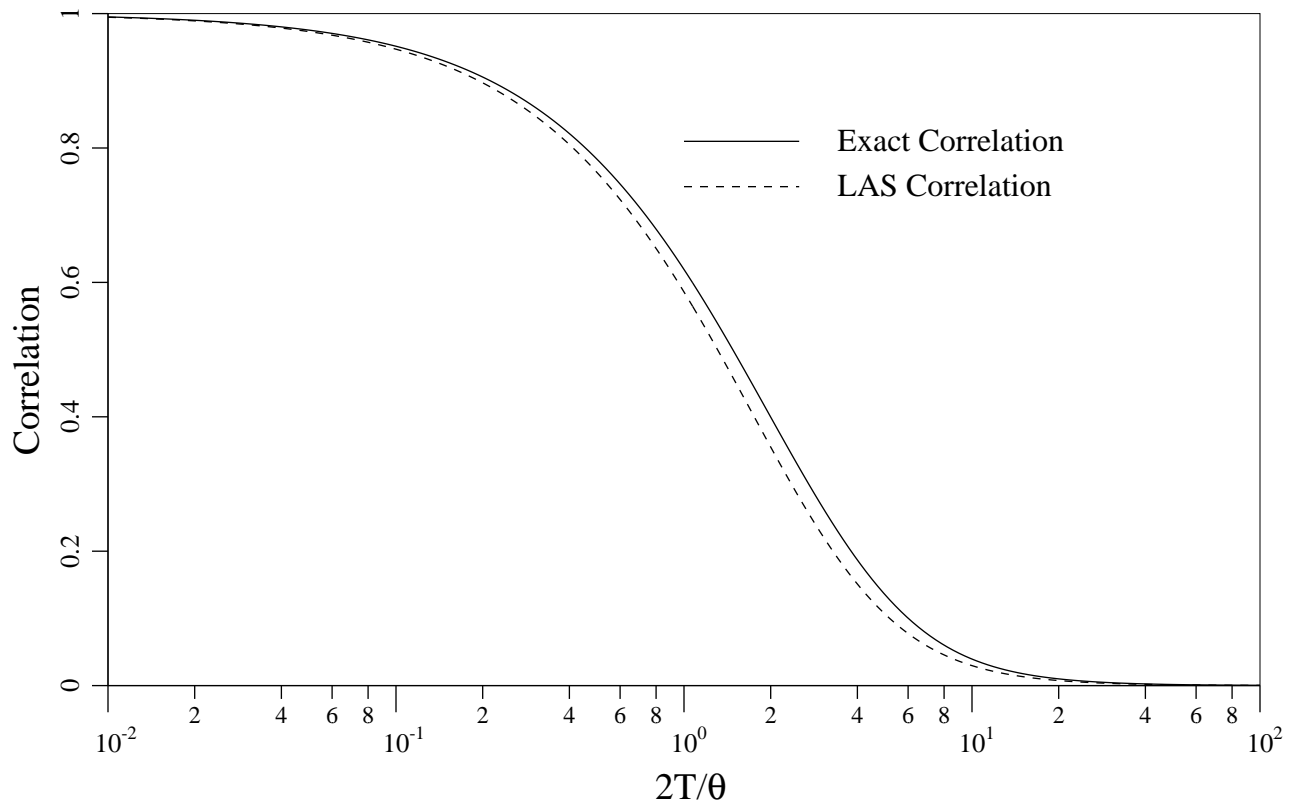


Figure 4 (Fenton/VanMarcke)

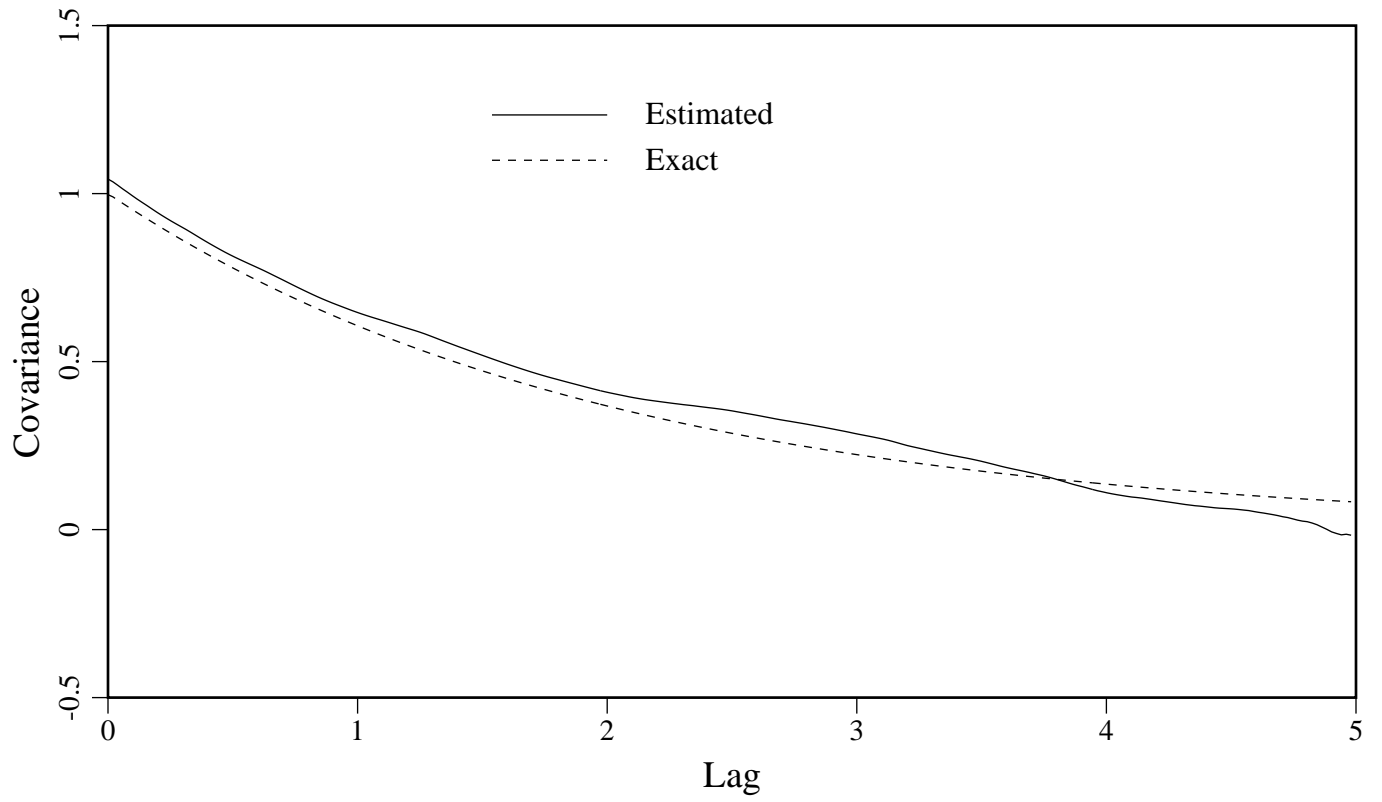


Figure 5 (Fenton/VanMarcke)

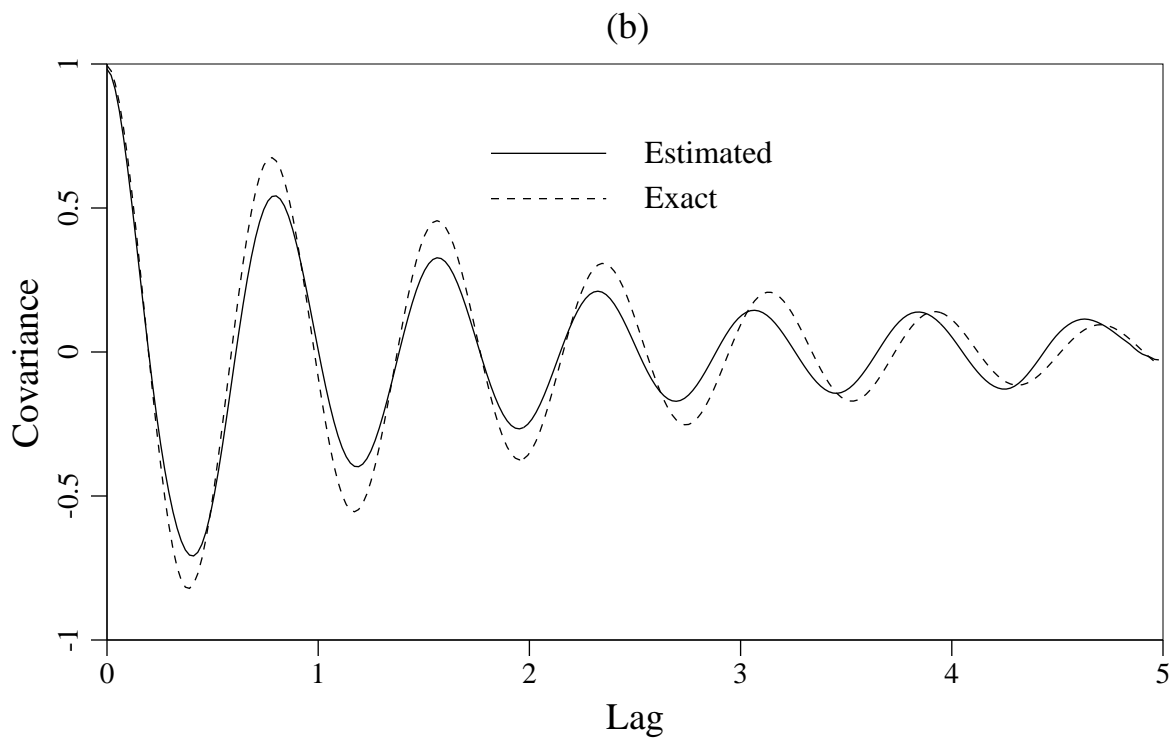
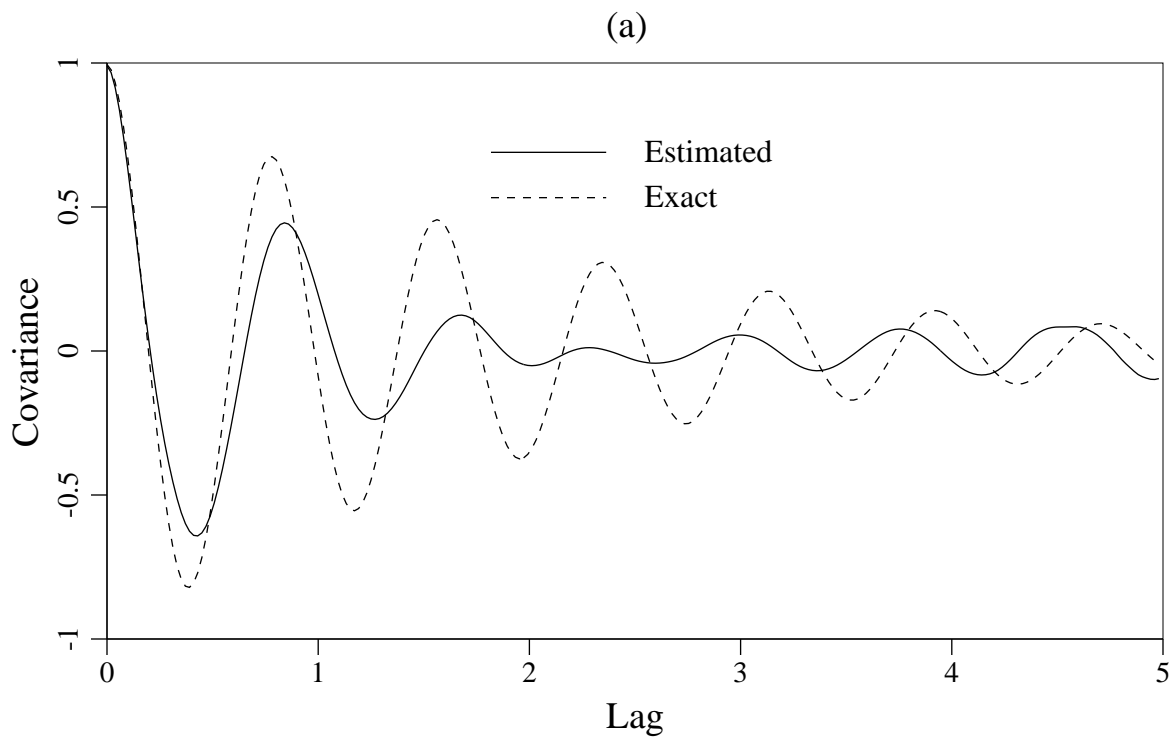


Figure 6 (Fenton/VanMarcke)

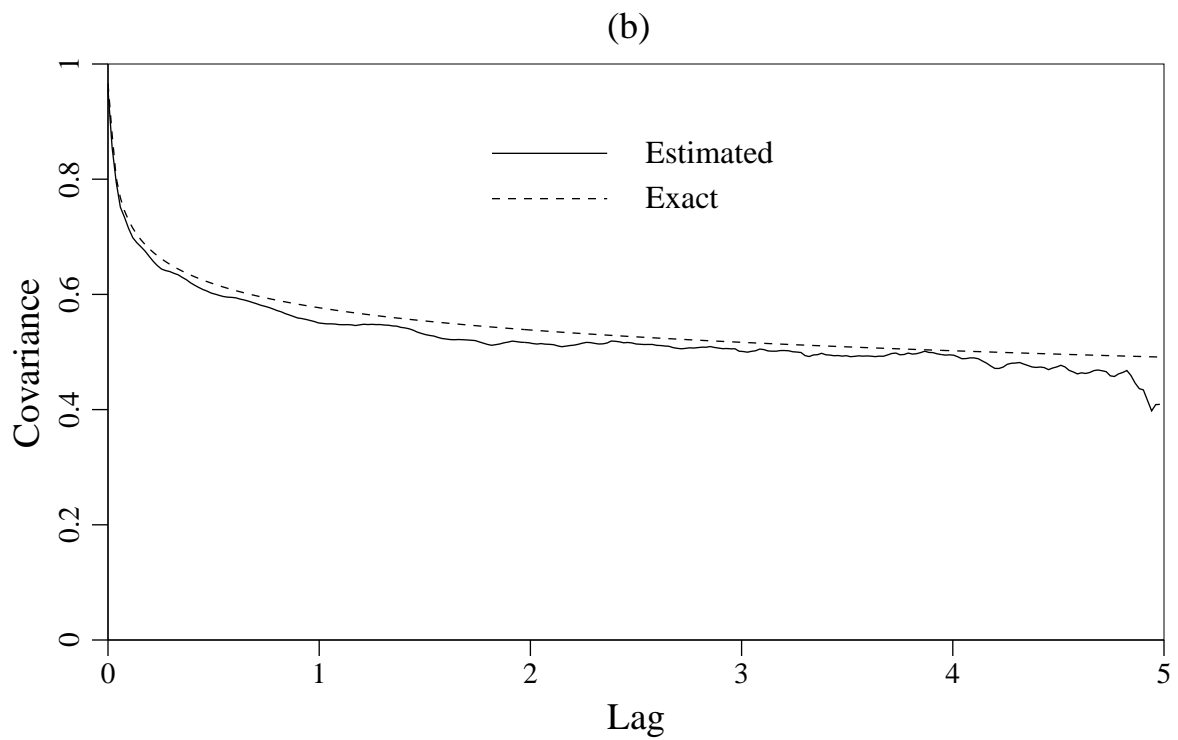
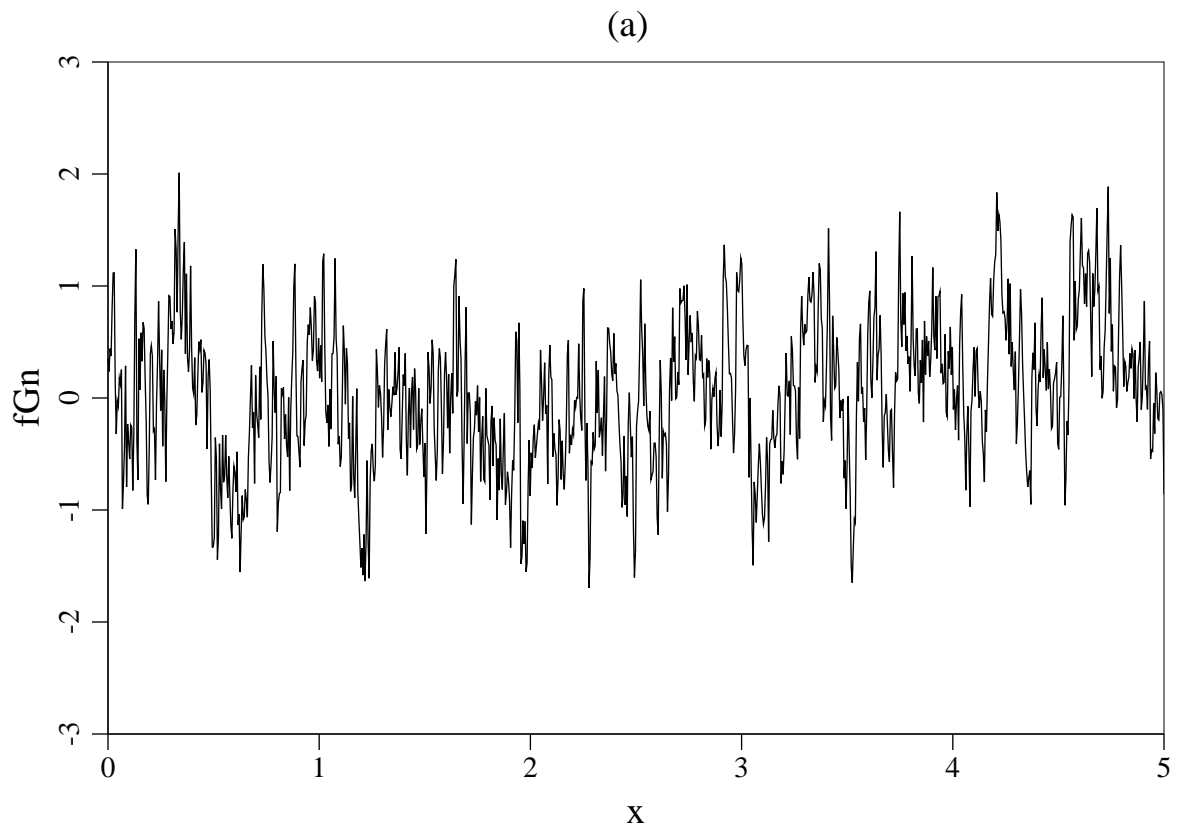


Figure 7 (Fenton/VanMarcke)

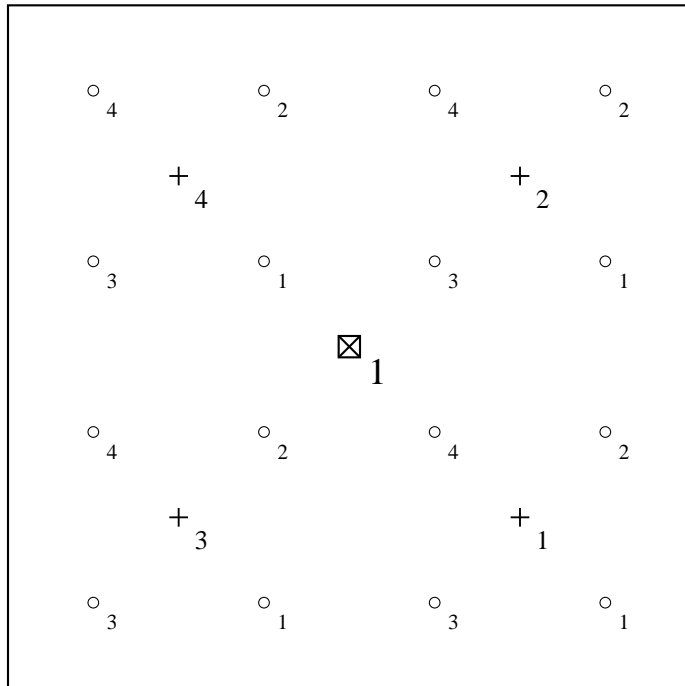


Figure 8 (Fenton/VanMarcke)

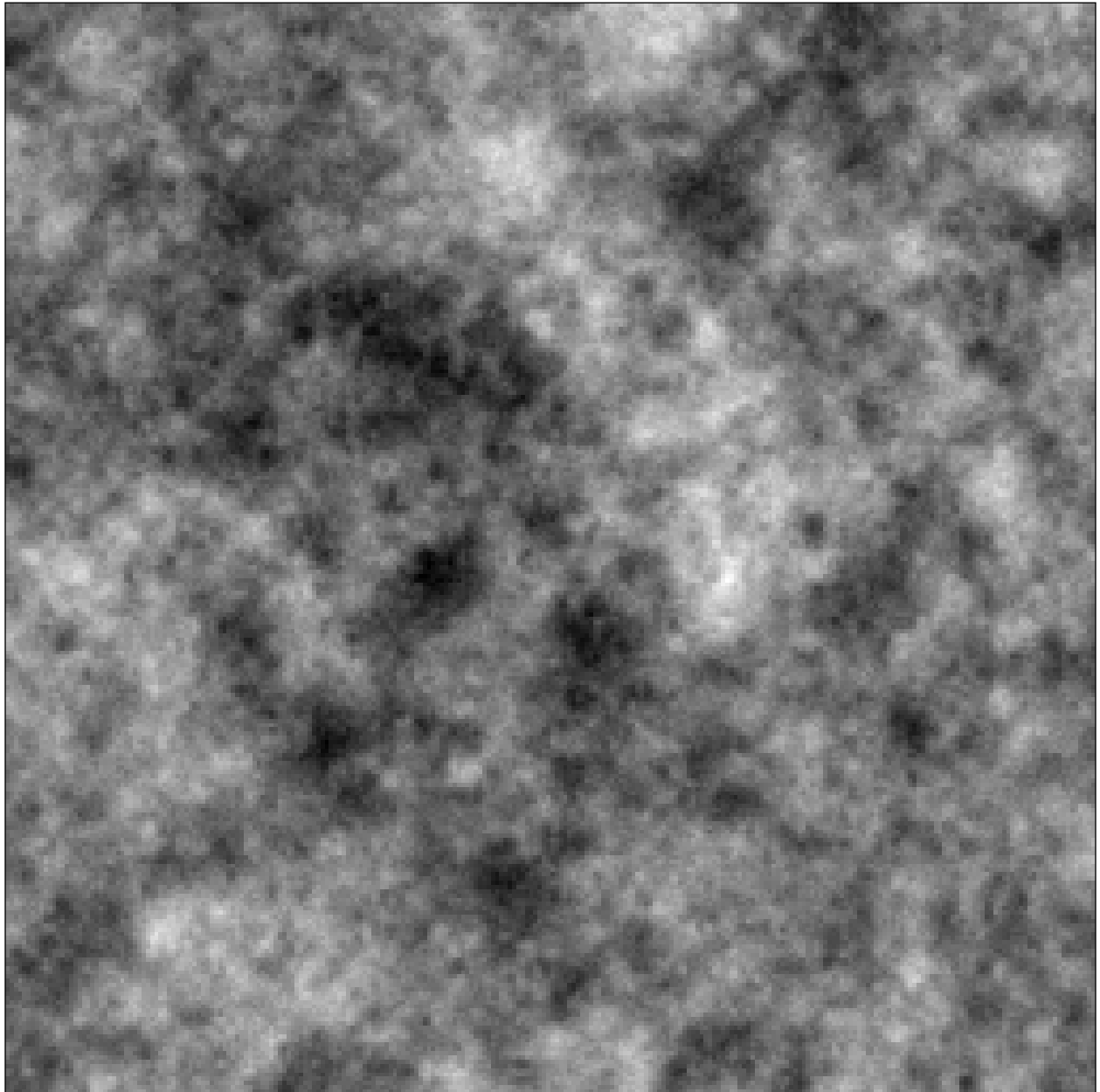


Figure 9 (Fenton/VanMarcke)

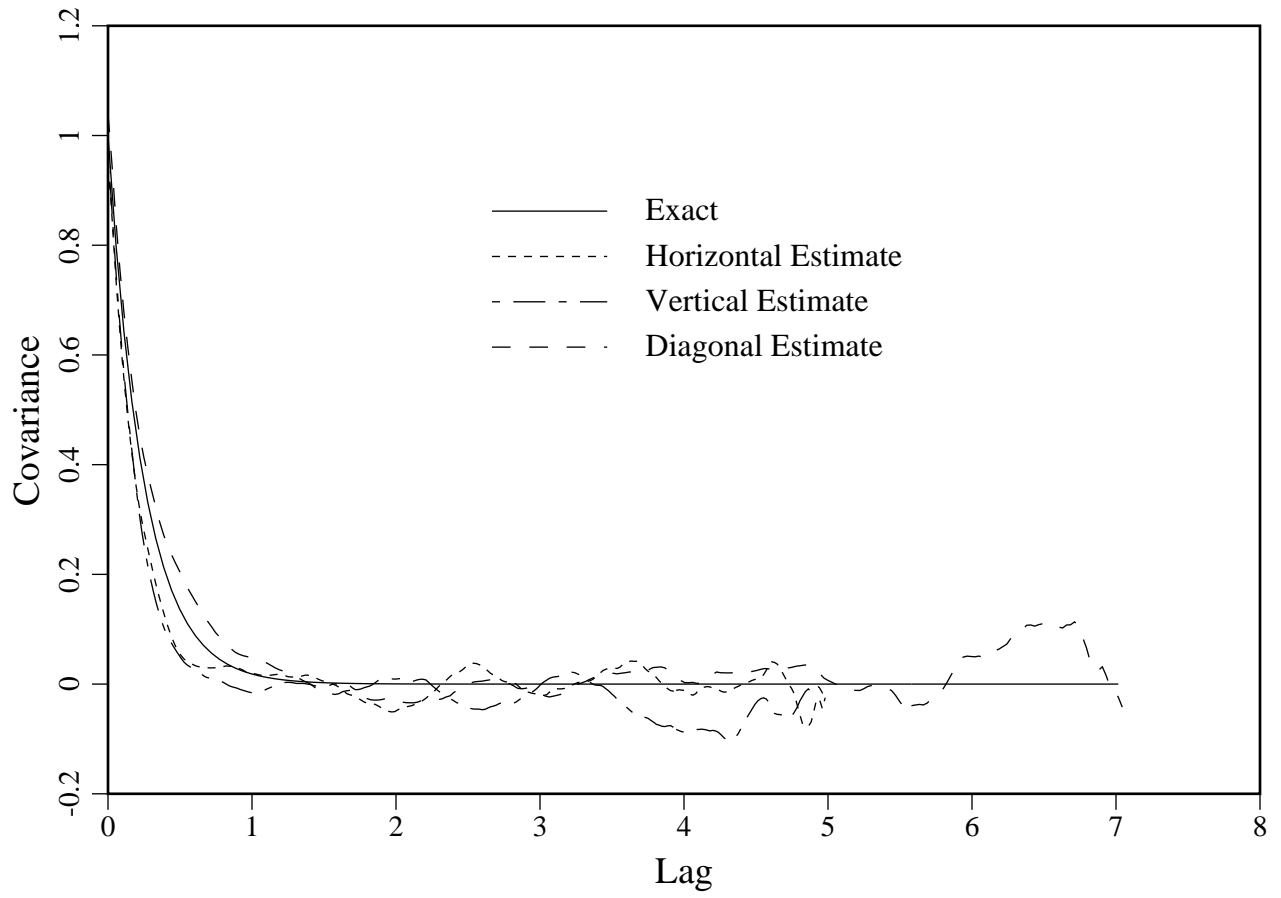


Figure 10 (Fenton/VanMarcke)

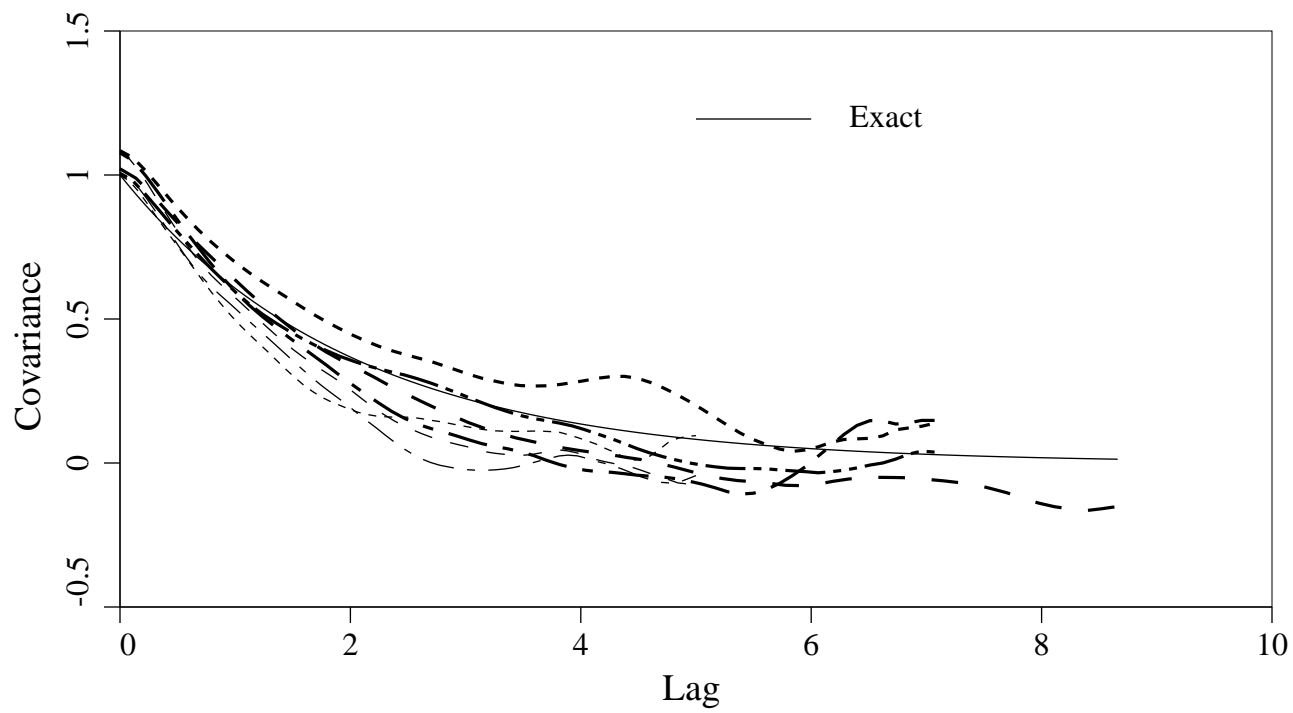


Figure 11 (Fenton/VanMarcke)